A piRNA regulating oogenesis and embryo development in cockroaches

Judit Gonzalvo[1]*, Nuria Farrus[1]*, Jorge Escudero[1]*, David Pujal[1], Josep Bau[2], Maria-Dolors Piulachs[1§]

[1] *Institute of Evolutionary Biology (CSIC-University Pompeu Fabra). Passeig Marítim de la Barceloneta, 37. 08003 Barcelona, Spain*

[2] *Department of Biosciences, University of Vic - Central University of Catalonia. Barcelona, Spain*

[§]Corresponding author: Maria Dolors Piulachs (mdolors.piulachs@ibe.upf-csic.es)

*These authors contributed equally to this work.

Keywords

insect reproduction, sncRNA, insect ovary, ASO, PIWI, ecdysone, *Blattella germanica*, embryogenesis

Abstract

The PIWI-interacting RNAs (piRNAs) are small non-coding RNAs ranging from 26 to 31 nucleotides. Initially, piRNA functions were associated with repressing transposable elements as part of a mechanism that maintains genomic stability across evolution. However, in the last years, new regulatory functions for piRNAs have been identified. Now, we investigated the regulatory role of piRNAs in insect oogenesis and embryo development. We studied the expression and function of piRNA-83679, one the most abundantly expressed piRNA in *Blattella germanica* adult ovaries. piRNA-83679 is expressed in germinal and somatic cells in adult ovaries during the gonadotropic cycle, and is maternally provided to the egg. Using an antisense oligonucleotide (ASO), we reduced piRNA-83679 levels in *B. germanica* adult females, enabling the study of its

functions. piRNA-83679 depletion affected the expression of different ecdysone and chorion genes in the ovary, and the organization of the F-actin fibers in the basal pole of the follicle cells of the basal ovarian follicle. As a result, the eggs were not correctly encapsulated in the ootheca. Moreover, piRNA-83679 depletion delayed oviposition and affected embryo development, especially in the early stages.

Introduction

The piwi-interacting RNAs (piRNAs) are small non-coding RNAs (sncRNAs) ranging from 26 to 31 nt in length, whose biogenesis is associated with PIWI proteins subfamily (Hirakata and Siomi, 2016; Le Thomas et al., 2014). In terms of sequence, piRNAs are poorly conserved even among closely related species, which suggest function specificity (Aravin et al., 2007; O'Donnell and Boeke, 2007; Wang et al., 2019). Two pathways of piRNA biogenesis have been described in *Drosophila melanogaster*, the primary pathway involves somatic cells, whereas the secondary, also known as the "ping-pong" pathway, involves germ cells. All together silence the expression of transposons, both transcriptionally and post-transcriptionally (Gleason et al., 2018; Hirakata and Siomi, 2016). However, evidence obtained in other arthropods has shown that the two piRNA pathways operate in both somatic and germinal tissues (Cerqueira de Araujo et al., 2022; Yamashita et al., 2024).

The first function associated with piRNAs was the repression of transposable elements (TEs), as part of an evolutionarily conserved mechanism that ensures genomic stability in germ cells (Aravin et al., 2007; Senti et al., 2015). However, recent studies revealed the origin of some piRNAs in coding sequences, intergenic regions unrelated to TEs, and 5' and 3' untranslated regions (UTRs) of mRNAs, which suggest that piRNAs regulate gene expression (Iki et al., 2023; Jensen et al., 2020; Lambert et al., 2019; Rojas-Ríos et al., 2018). In this sense, piRNA functions related to embryogenesis, germ cell specification, primary sex determination and epigenetic states, have been described (Gleason et al., 2018; Gou et al., 2014; Iki et al., 2023; Kiuchi et al., 2014).

In a previous study on the cockroach *Blattella germanica*, we reported a significant number of piRNAs maternally provided to the zygote, which are abundant in early

embryo (Belles et al., 2024; Llonga et al., 2018). In the present work we approached the functional study of one of these piRNAs by depleting its expression with an antisense oligonucleotide (ASO). ASOs are short (18-30 nt) single-stranded DNA molecules that can bind specifically RNA to modulate gene expression (Roberts et al., 2020). ASOs have been used in medicine since late 1970 as therapeutics against different illnesses, as they can be designed with great specificity against their mRNA targets (Crooke et al., 2021). ASOs can bind to the corresponding mRNA target by Watson–Crick base pairing, forming an RNA-DNA heteroduplex which invokes the RNAse-H endonuclease to cleave and ultimately reduce the levels of the target RNA. Despite their demonstrated potential, ASOs have barely been used to regulate insect gene expression (Oberemok et al., 2018).

B. germanica has the panoistic ovary type, in which all stem cells in the germline are converted into functional oocytes, with transcriptionally active nuclei (Bu□ning, 1994). During *B. germanica* oogenesis, only the basal oocyte of each ovariole matures in every gonadotropic cycle, while the other oocytes remain arrested in the vitellarium until the onset of the next cycle (Irles and Piulachs, 2014; Rumbo et al., 2023). Once released from the germarium, the oocyte is surrounded by a monolayer of follicular cells (FCs), thus establishing an ovarian follicle (Rumbo et al., 2023). The FCs mature and change their characteristics in parallel to oocyte growth. When the basal ovarian follicle (BOF) begins to mature, in the sixth (last) nymphal instar, the FCs proliferate, increasing their number until covering the entire oocyte (Irles and Piulachs, 2014). Later, in 3-day-old adult, cytokinesis in FCs is arrested, and cells become binucleated. Under the control of the juvenile hormone circulating in the hemolymph, the FCs contract the cytoplasm thus leaving large intercellular spaces (Davey, 1981; Davey and Huebner, 1974), which facilitate the access of vitellogenin to the oocyte membrane. Henceforth, the oocytes in the BOFs grow exponentially. At the end of the gonadotropic cycle, the FCs in the BOF close definitively the intercellular spaces (Belles et al., 2024) and chorion synthesis begins. This step is induced by the ecdysone production in the ovary (Bellés et al., 1993; Pascual et al., 1992), taking few hours (Irles et al., 2009b). Several genes involved in the biosynthesis of ecdysone have been characterized in the ovary of *B. germanica*, namely *neverland* (*nvd*), *spook* (spo), *spookiest* (*spot*), *phantom* (*phm*), *disembodied* (*dib*),

shadow (*sad*) and *shade* (*shd*) (Belles et al., 2024). The action of ecdysone also involves *E75*, an early gene in the ecdysone signaling cascade, and *fushi tarazu- f1* (*ftz-f1*), a late gene that also regulates the expression of ecdysteroidogenic genes, and helps to maintain the correct cytoskeleton organization in the BOF at the end of the gonadotropic cycle (Alborzi and Piulachs, 2023). Regarding chorion formation, two genes have been thoroughly characterized in *B. germanica*: *citrus* (Irles and Piulachs, 2011) and *brownie* (*brw*) (Irles et al., 2009a). At the end of choriogenesis, the cytoskeleton of the follicular epithelium of the BOFs is rearranged thus facilitating the egg release into the oviduct (Alborzi and Piulachs, 2023). The eggs are then oviposited into a hard egg capsule or ootheca. In B. germanica, the female transports the ootheca attached to the genital atrium during all the embryogenesis, which lasts eighteen days under our laboratory conditions (Belles et al., 2024).

2. Materials and methods

2.1. *B. germanica* colony and tissue sampling

Newly emerged *B. germanica* adult females, were obtained from a colony fed *ad libitum* on Panlab 125 dog food and water, maintained in darkness at 29 ± 1 °C and 60-70% relative humidity (Bellés et al., 1987). All dissections were performed on CO_2 anesthetized specimens. In adult females, the length of the BOF was used to establish chronological age. Females were maintained with males and, at the end of each experiment, the presence of spermatozoa in the spermatheca was assessed to confirm fertility.

2.2. Small RNA library processing

B. germanica piRNA sequences were obtained from small RNA libraries previously prepared in our laboratory (Ylla et al., 2017) (publicly available at GEO: GSE87031). They correspond to different developmental stages, including ovaries from 7-day-old adults, non-fertilized eggs, embryos (days 0, 1, 2, 6 and 13) and nymphs (instars 1, 3, 5 and 6). The small RNA libraries were preprocessed to remove sequencing adapters using Trimmomatic (v 0.39, as relevant parameters: ILLUMINACLIP TruSeq2-

PE.fa:2:15:10 LEADING:20 MINLEN:18) (Bolger et al., 2014). Reads between 26 and 31 nucleotides were selected with Cutadapt (v 3.5) (Martin, 2011) and aligned to the *B. germanica* genome assembly (v 1.1) (Harrison et al., 2018) with Bowtie2 (v 2.4.4, as relevant parameters: -a --end-to-end --score-min L,0,0) (Langmead and Salzberg, 2012), resulting in 2,534,205 aligned putative piRNA sequences. Infrequent sequences were filtered out by applying a cut-off of 17 reads, reducing the number of sequences to 128,653. Finally, the sequences that shared the same genomic 5' start position and only differed in their length at the 3' end were collapsed. The counts of each of the collapsed variants were attributed to the most expressed one, and were normalized using the median-of-ratios method from DESeq2 (Love et al., 2014). The data obtained was used to select the piRNA candidate for functional studies.

2.3. RNA extraction and expression studies

The extraction of ovarian small RNAs was carried out at different ages using the miRNAeasy Mini Kit (Qiagen), following the manufacturer's protocol. The quantity and quality of the extracted small RNAs were estimated by spectrophotometric absorption at 260/280 nm using a Nanodrop spectrophotometer (MicroDigital Co, Ltd). A total of 400 ng of each RNA extraction was reverse transcribed with the 1st Strand cDNA synthesis Kit (Agilent Technologies) to obtain cDNA. The forward primer used in qRT-PCR was designed using the full sequence of the piRNA. The universal primer from the Agilent 1st Strand cDNA synthesis Kit was used as the reverse primer. The efficiency of the primers used in qRT-PCR was first validated by constructing a standard curve through three serial dilutions of cDNA from ovaries (Figure S1). The *U6* small nuclear RNA was used as a reference for expression studies (Tanaka and Piulachs, 2012). qRT-PCR reactions were performed with iTaq Universal SYBR Green Supermix (Bio-Rad Laboratories). Amplification reactions were performed at 95 °C for 5 min, 44 cycles of 95 °C for 10 s plus 62 °C for 40 s, followed by 95 °C for 1 min and finally, the melting curve: from 60 °C to 95 °C with a measurement every 0.5 °C increase. After the amplification phase, a dissociation curve was carried out to ensure that there was only one product (Figure S1).

Total RNA extraction from 7-day-old adult *B. germanica* ovaries was carried out using Tissue Total RNA purification Kit (Canvax Biotech), following the manufacturer's protocol. The quantity and quality of the extracted RNAs were estimated by spectrophotometric absorption at 260/280 nm using a Nanodrop spectrophotometer (MicroDigital Co, Ltd). A total of 200 ng of each RNA extraction was reverse-transcribed using the Transcriptor First Strand cDNA Synthesis Kit (Roche) to obtain the corresponding cDNAs. The expression of selected mRNAs related to the studied processes was determined by qRT-PCR, using iTaq Universal SYBR Green Supermix (Bio-Rad Laboratories), and *actin-5c* mRNA expression as a reference. The amplification reactions were performed at 95 °C for 3 min, 44 cycles of 95 °C for 10 s plus 57 °C for 1 min, followed by 95 °C for 10 s and finally, the melting curve: from 57 °C to 95 °C with a measurement at each 0.5 °C increase.

Expression levels of small RNAs and mRNAs were calculated relative to their respective reference gene, using the 2-ΔCt method (Irles et al., 2009b; Livak and Schmittgen, 2001). Results are given as copies of small RNA per 1000 copies of *U6*, or copies of mRNA per 1000 copies of *actin-5c* mRNA and correspond to three biological replicates. The primer sequences are detailed in Table S1**.**

2.4. Treatments with antisense oligonucleotides

The piRNA-83679 levels were reduced using a chemically unmodified antisense oligonucleotide (ASO: 5'-GGAGGTCCCCCAGACCGGCACAGACCGAA-3') designed over the entire piRNA sequence. Newly emerged adult females were treated with 1 µL of a solution of 15 µg/µL of ASO in water (from now on ASO-treated). As negative control, the same dose of an oligonucleotide custom-designed (ASO-Control) was administered. The sequence of ASO-Control correspond to the sequence of the recognition sites of 5 restriction enzymes concatenated (XbaI, HindIII, KpnI, BamHI), and four nucleotides more to reach the same length than the ASO: 5'-TCTAGAAAGCTTGGTACCGGATCCCAGGT-3'). Alternatively, both water and ASO-Control were used in control animals since no significant differences were observed in oviposition rates or the number of emerged nymphs. (ASO: 40.27 ± 1.161 nymphs (n

= 15); Water: 42.25 ± 0.75 nymphs (n = 12); p-value: 0.187), from now on, referred as Mock-treated.

2.5. Microscopy methodologies

2.5.1. In situ hybridization

The piRNA-83679 was localized in ovaries from *B. germanica* adults using an antisense LNA (locked nucleic acid) probe conjugated to Digoxigenin (DIG) at the 5' and 3' ends (5'-DIG-GGAGGTCCCCCAGACCGGCACAGACCGAA-DIG-3', Merck). Ovaries were dissected under Ringer's saline, and immediately fixed in paraformaldehyde (4% in PBS 0.2 M; pH 6.8) overnight. Subsequent hybridization and washing reactions were carried out as previously reported (Irles et al., 2009b). The DIG hapten was detected by incubating the samples in a 1:4,000 dilution of anti-DIG-rhodamine antibody (Roche, Basel, Switzerland) in PBS-T for 90 min at room temperature. Ovaries were washed again and incubated in DAPI (4',6-diamidino-2-phenylindole 1 µg/mL, Merck) for 5 min at room temperature.

2.5.2. DAPI-TRITC-Phalloidin staining

Ovaries from 7-day-old *B. germanica* adults, were dissected under Ringer's saline, and immediately fixed in paraformaldehyde (4% in PBS 0.2 M; pH 6.8) for two hours. Subsequently, they were washed with PBT (PBS 0.2 M; pH 6.8 + 0.2% Tween-20) (Irles and Piulachs, 2014). The ovaries were incubated for 20 min in 300 ng/mL of TRITC-phalloidin (tetramethylrhodamine isocyanate-phalloidin, Merck) prepared in PBT, and after washing with PBT, were incubated for 5 min in 1 µg/mL of DAPI, and washed again with PBT.

Samples were mounted with Mowiol (Calbiochem) and analyzed by epifluorescence using a Zeiss AxioImager.Z1 microscope (Apotome) (Carl Zeiss MicroImaging).

2.5.3. Embryo observations

Fifteen-day-old oothecae were removed from the female abdomen by gentle pressure, in order to observe the embryo development. The oothecae were incubated during 5 min in water at 95 °C to facilitate the individualization of the embryos. Images of embryos were obtained using a Zeiss DiscoveryV8 stereomicroscope (Carl Zeiss MicroImaging).

2.6. Statistical analysis

The data are expressed as mean ± standard error of the mean (S.E.M.). Statistical analyses were performed using GraphPad Prism version 8.1.0 for Windows, GraphPad Software. The significant differences between control and treated groups was calculated using the Student's t-test. The data were evaluated for normality and homogeneity of variance using the Shapiro–Wilk test, which showed that no transformations were needed. All datasets passed normality test.

Results

3.1. piRNA-83679 in the ovary

B. germanica piRNAs were ranked according to their levels in the transcriptomes of both 7-day old adult ovaries and non-fertilized eggs. As candidate for functional studies, we selected the piRNA-83679 (5'-UUCGGUCUGUGCCGGUCUGGGGGACCUCC-3'), showing quite high levels in non-fertilized eggs, which suggests that it is maternally transmitted (Figure 1A). piRNA-83679 levels are still detected in early embryonic stages (embryos day 0 to day 2), but it is undetectable in later embryo stages and in early nymphal instars (Figure 1A). piRNA-83679 levels reappear in the last nymphal instars, although at considerably low levels (Figure 1A).

In *B. germanica* adult ovaries, piRNA-83679 increase gradually as the BOF grows and matures. In the transition from 3- to 4-day-old females, piRNA-83679 levels are doubled (Figure 1B), coinciding with changes in the program of FCs in the BOF, which become binucleated (Irles and Piulachs, 2014). From day 4, piRNA-83679 levels tend to decrease, increasing again on day 7 and reaching the highest levels, concurrently with the synthesis of the chorion proteins by the FCs (Figure 1B) (Irles et al., 2009b). *In situ* hybridization observations led to the localization of piRNA-83679 in the FCs of the adult

female BOF. Labeling appeared accumulated in the cytoplasm of FCs early in the gonadotropic cycle (Figure 1C). In 5-day-old females, piRNA labeling was still detected in the cytoplasm of the FCs (Figure 1D), with an increase of the labeling close to the nuclei membrane (Figure 1D, white arrow). Due to the big size of the BOF in 5-day-old females, we were not able to observe labeling inside the basal oocyte. However, in subbasal ovarian follicles, piRNA-83679 labelling was detected in the oocyte cytoplasm and nucleus, showing an increasing signal towards the anterior and posterior oocyte poles (Figure 1E, arrowheads).

3.2. piRNA-83679 and basal ovarian follicle development

To study the function of piRNA-83679, newly emerged *B. germanica* adult females were treated with an ASO targeting the piRNA, and effects were observed 7 days after the treatment.

In 7-day-old Mock-treated adult females, the binucleated FCs in the BOF, have a uniform distribution, with nuclei having the same size and shape (Figure 2A, E) and begin to close intercellular spaces (Figure 2A, arrows). Once the chorion is completed the actin cytoskeleton surrounds the FCs, modifying their distribution, covering the surface of the basal pole of FCs in an organized manner, and packing the entire ovarian follicle (Figure 2B). Just before ovulation, the actin fibers wrap up the FC, giving them a rounded shape (Figure 2C), allowing the contractions of the ovarian follicle that facilitate ovulation and oviposition.

piRNA-83679 levels in the ovaries were quantified in 7-day-old adult Mock- and ASO-treated females. Results showed that piRNA-83679 levels in ASO-treated females were significantly lower ($p = 0.0107$) compared to Mock-treated females (Figure 2D). The comparison of FCs from the BOF of ASO-treated females with controls evidenced some morphological changes. These FCs of piRNA-83679-depleted females had big nuclei, heterogeneous in shape with bizarre morphologies (Figure 2F). Moreover, the distribution of the F-actin fibers in the basal pole of the FCs was disorganized (Figure 2G). The fibers did not follow the correct orientation on the ovarian follicle surface, overloading different FCs.

Relevant changes in the mRNA levels of ecdysteroidogenic genes were detected (Figure 2H). The expression of *nvd* remained unaffected by the treatment. Conversely, the expression of *spo* increased significantly by 41% ($p = 0.0003$), while the expression of *phm*, *dib*, and *sad* tended to increase, but differences regarding the controls were not statistically significant (Figure 2H). Interestingly, the expression of *shd*, which encodes a 20-hydoxylase responsible for converting ecdysone into its active form, 20-hydroxyecdysone (20E), tended to decrease by an average of 61% (Figure 2I). In turn, the lower availability of 20E determined by the low expression of *shd*, apparently resulted in a significant reduction of *E75A* (71%, $p = 0.03$, Figure 2I) and a dramatic depletion of *ftz-f1* transcripts (94%, $p = 0.02$, Figure 2I). These changes in ecdysone signaling also resulted in a significant and dramatic depletion of the chorion genes *citrus* and *brw* (99.89% and 99.95 % respectively, $p < 0.0001$; Figure 2I).

3.3. piRNA-83679 function on reproduction and embryo development

To further our study, we wondered whether depletion of piRNA-83679 in the adult female could affect reproduction and embryo viability. Again, newly emerged adult females were treated with the same ASO targeting the piRNA, and the insects were paired with males and left until ootheca formation. The first effect observed was a significant delay in oviposition in the ASO-treated females (8.11 ± 0.26 days; $n = 53$; $p = 0.013$), compared to Mock-treated insects (7.33 ± 0.08 days; $n = 38$).

Despite this delay, ASO-treated females transported the ootheca during the entire embryogenesis period (18.50 ± 0.26, $n = 32$) without differences compared to controls (18.81 ± 0.21, $n = 28$). However, although all the ASO-treated females were mated ($n = 32$), a significant number (25%, $n = 8$) of oothecae did not give nymphs. In the rest of ASO-treated females, the number of hatching nymphs was significantly reduced (36.29 ± 1.60; $n = 24$) with respect to Mock-treated females (41.15 ± 0.74; $n = 27$; $p = 0.0062$). The reduced number of hatching nymphs may be related to the fact that several ASO-treated females (31.25%, $n = 10$) produced defective oothecae, shorter, curved, dried, or a combination of the three defects, which often resulted in eggs not well aligned (Figure 3A and B) that compromised hatching. The number of hatching nymphs from these

malformed oothecae was greatly reduced (24.25 ± 3.64 nymphs; n = 4) or they did not give any nymphs (n = 6). (Figure 3B).

Fifteen-day-old oothecae from Mock- and ASO-treated females were opened to observe the embryos and analyze how piRNA-83679 depletion affected development. At this age, embryos from Mock-treated females (94 embryos from 4 oothecae) had completed the dorsal closure, and the tips of the antennae and the hind legs almost reached the seventh abdominal segment. Eye coloring is completed, and mandibles and legs sclerotization is at the onset (Figure 3C) (Piulachs et al., 2010; Tanaka, 1976). In contrast, embryos from ASO-treated females (107 embryos from 3 oothecae) exhibited a wide range of phenotypic defects. A large percentage of embryos were morphologically similar to controls but less sclerotized (62% of embryos) (Figure 3D). The phenotypes of the remaining 38% embryos ranged from eggs that had not formed the germinal band, having the aspect of an amorphous mass (Figure 3E), to embryos with segmentation not completed and with defective eyes (Figure 3F, G). There were embryos without pigmentation in the eyes (Figure 2F), while others had eyes of incorrect shape (Figure 2H). In these group of embryos, the dorsal organ was still visible (Figure 2H, arrow). In addition, none of these embryos showed signs of sclerotization in the appendages, and, in general, the legs did not have the correct size and shape (Figure 2F-I). Also, in few ASO-treated embryos, the fat body cells (urate cells and mycetocytes, see A. Tanaka, 1976), were more abundant than in Mock-treated ones (Figure 2I, white dots in the thorax and abdomen).

4. Discussion

The role of piRNAs as regulators of TEs and protectors of the genome is an established function. However, research published in recent years has shown the importance of piRNAs as mRNA regulators. Thus, piRNA functions have been extended to processes as different as the maintenance of germinal stem cells, DNA repair mechanisms, sex determination, chromatin modifications, learning and memory, and cancer mechanisms (Gleason et al., 2018; Iki et al., 2023; Kiuchi et al., 2023, 2014).

Insect oogenesis is a highly regulated process that involves multiple steps and processes: germ cell proliferation, oocyte growth and maturation, vitellogenesis, and eggshell formation. All of these processes occur under the control of ecdysone and juvenile hormone (Alborzi and Piulachs, 2023; Belles et al., 2024). Moreover, given the efficiency and precision required, the regulation implies different regulatory layers, involving proteins, mRNAs, and non-coding RNAs, which have specific functions at different regulatory levels. Among the non-coding RNAs there are the small non-coding RNAs and among them the piRNAs.

We have found that the piRNA-83679 is highly expressed in *B. germanica* ovary, being present in somatic and germinal cells. In addition, piRNA-83679 levels in the ovary correlate with the main changes in the BOF, which are mainly related to the changes in the FCs program (Claycomb and Orr-Weaver, 2005; Irles et al., 2016, 2009b; Irles and Piulachs, 2014, 2011). piRNA-83679 expression changes in critical moments, like those related to the arrest of cytokinesis, increase of polyploidy, or the endoreplication in the FCs, suggest a role in protecting the genome. However, piRNA-83679 must play other functions since it is maternally provided to the embryo.

Using an ASO to deplete the piRNA-83679 allowed us to infer its functions in the adult insect ovary and the embryo. Reduction of piRNA-83679 levels in the ovary led to a delay in oviposition and malformations in the ootheca shape and size. These ootheca defects could explain the observed reduction in the number of emerging nymphs. Moreover, the expression profile of the piRNA-83679 in the ovary, and the oothecae malformation produced when reducing the levels of the piRNA-83679, suggest an effect of this piRNA on genes important at the end of the gonadotropic cycle, among them, ecdysteroidogenic genes expressed in the adult ovary. In most adult insects, when the prothoracic gland degenerates, the ovary becomes the main source of ecdysone, which acts then in an autocrine way (Pascual et al., 1992; Romaña et al., 1995). In *B. germanica* adults, ecdysone is mostly necessary at the end of the gonadotropic cycle to facilitate the endoreplication of some genome regions in the FCs, promoting chorion synthesis and facilitating the release of the egg to the oviduct (Alborzi and Piulachs, 2023; Belles et al., 2024; Belles et al., 1993). Depletion of piRNA-83679 resulted in a depletion of *shd* mRNA expression, which prevents the transformation of ecdysone to

20E., resulting in an overexpression *phm*, *dib*, and *sad*. This suggests that piRNA-83679 directly or indirectly represses the expression of these three genes, or that the mRNAs of these three genes were accumulated due to the *shd* reduction.

As ecdysone is not transformed into 20E due to *shd* depletion the transduction of the 20E signal becomes hampered, as shown by the low levels of *E75A* expression. Then the attenuation of 20E signaling affects the FCs program in the BOFs (Ramos et al., 2020), which in turn results in a decrease in the expression of chorion genes. Since the piRNAs have been described as repressors of mRNAs, the reduction of *shd* expression determined after the ASO treatment suggests that piRNA-83679 would inhibit a *shd* repressor.

The cytoskeleton of the BOF, which contributes to the release of the egg to the oviduct was also affected by the piRNA-83679 depletion. We had previously described that in *B. germanica* ovaries *ftz-f1* contributes to control the distribution of the cytoskeleton and its organization at the end of the gonadotropic cycle (Alborzi and Piulachs, 2023). Now, we have observed that piRNA-83679-depleted females show a reduction of ftz-f1 levels. This reduction resulted in the same phenotype obtained when *ftz-f1* was depleted by RNAi in adult females, which involved a decrease in ecdysone levels (Alborzi and Piulachs, 2023).

The diversity of phenotypes resulting from piRNA depletion could be attributed to its action on different mRNA targets. It is worth noting that the functions described here may be only part of the functions of ovarian piRNA-83679 in *B. germanica*. Thus, maternal provision of piRNA-83679 to the embryo suggests that it would play specific roles in early embryo development and future work will be done in this way. In any case, our results show that the use of ASOs to deplete piRNAs can be a useful approach to study the functions of these still mysterious sncRNAs.

Acknowledgments

We thank the financial support to the project PID2021-122316OB-I00 from the MCIN/AEI/ 10.13039/501100011033 and by ERDF, a way of making Europe, and to the Catalan Government (2021 SGR 00419). This work was supported by Pla de Doctorats

Industrials de la Secretaria d'Universitats i Recerca del Departament d'Empresa i Coneixement de la Generalitat de Catalunya (grant number 2021 DI 059). The authors acknowledge the support of the publication fee by CSIC Open Access Publication Support Initiative through its Unit of Information Resources for Research (URICI).

References

Alborzi, Z., Piulachs, M.D., 2023. Dual function of the transcription factor Ftz-f1 on oviposition in the cockroach Blattella germanica. Insect Mol. Biol. 32, 689–702. https://doi.org/10.1111/imb.12866

Aravin, A.A., Hannon, G.J., Brennecke, J., 2007. The Piwi-piRNA pathway provides an adaptive defense in the transposon arms race. Science 318, 761–4. https://doi.org/10.1126/science.1146484

Bellés, X., Casas, J., Messeguer, A., Piulachs, M.D., 1987. In vitro biosynthesis of JH III by the corpora allata of adult females of Blattella germanica (L). Insect Biochem. 17, 1007–1010. https://doi.org/10.1016/0020-1790(87)90111-9

Belles, X., Cassier, P., Cerdá, X., Pascual, N., André, M., Rósso, Y., Piulachs, M.D.D., 1993. Induction of choriogenesis by 20-hydroxyecdysone in the german cockroach. Tissue Cell 25, 195–204. https://doi.org/10.1016/0040-8166(93)90019-H

Belles, X., Maestro, J.L., Piulachs, M.-D., 2024. The German cockroach as a model in insect development and reproduction in an endocrine context. Adv. In Insect Phys. 66, 1–47. https://doi.org/https://doi.org/10.1016/bs.aiip.2024.03.001

Bolger, A.M., Lohse, M., Usadel, B., 2014. Trimmomatic: a flexible trimmer for Illumina sequence data. Bioinformatics 30, btu170-. https://doi.org/10.1093/bioinformatics/btu170

Bu□ning, J., 1994. The Insect Ovary□: Ultrastructure, previtellogenic growth and evolution. Springer Netherlands.

Cerqueira de Araujo, A., Huguet, E., Herniou, E.A., Drezen, J.M., Josse, T., 2022. Transposable element repression using piRNAs, and its relevance to endogenous viral elements (EVEs) and immunity in insects. Curr. Opin. Insect Sci. 50, 100876. https://doi.org/10.1016/j.cois.2022.100876

Claycomb, J., Orr-Weaver, T.L., 2005. Developmental gene amplification: insights into DNA replication and gene expression. Trends Genet 21, 149–162. https://doi.org/10.1016/j.tig.2005.01.009

Crooke, S.T., Baker, B.F., Crooke, R.M., Liang, X., 2021. Antisense technology: an overview and prospectus. Nat. Rev. Drug Discov. 20, 427–453. https://doi.org/10.1038/s41573-021-00162-z

Davey, K.G., 1981. Hormonal control of vitellogenin uptake in rhodnius prolixus stål. Am. Zool. 21, 701–705. https://doi.org/10.1093/icb/21.3.701

Davey, K.G., Huebner, E., 1974. The response of the follicle cells of Rhodnius prolixus to juvenile hormone and antigonadotropin in vitro. Can. J. Zool. 52, 1407–1412.

Gleason, R.J., Anand, A., Kai, T., Chen, X., 2018. Protecting and diversifying the germline. Genetics 208, 435–471. https://doi.org/10.1534/genetics.117.300208

Gou, L.-T., Dai, P., Yang, J.-H., Xue, Y., Hu, Y.-P., Zhou, Y., Kang, J.-Y., Wang, X., L, H., Hua, M.-M., Gou, S.-T., Dai, P., Yang, J.-H., Xue, Y., Hu, Y.-P., Zhou, Y., Kang, J.-Y., Wang, X., Li, H., Hua, M.-M., Zhao, S., Hu, S.-D., Wu, L.-G., Shi, H.-J., Li, Y., Fu, X.-D., Qu, L.-H., Wang, E.-D., Liu, M.-F., 2014. Pachytene piRNAs instruct massive mRNA elimination during late spermiogenesis. Cell Res. 24, 680–700. https://doi.org/10.1038/cr.2014.41

Harrison, M.C., Jongepier, E., Robertson, H.M., Arning, N., Bitard-Feildel, T., Chao, H., Childers, C.P., Dinh, H., Doddapaneni, H., Dugan, S., Gowin, J., Greiner, C., Han, Y., Hu, H., Hughes, D.S.T., Huylmans, A.K., Kemena, C., Kremer, L.P.M., Lee, S.L., Lopez-Ezquerra, A., Mallet, L., Monroy-Kuhn, J.M., Moser, A., Murali, S.C., Muzny, D.M., Otani, S., Piulachs, M.D., Poelchau, M., Qu, J., Schaub, F., Wada-Katsumata, A., Worley, K.C., Xie, Q., Ylla, G., Poulsen, M., Gibbs, R.A., Schal, C., Richards, S., Belles, X., Korb, J., Bornberg-Bauer, E., 2018. Hemimetabolous genomes reveal molecular basis of termite eusociality. Nat. Ecol. Evol. 2017 23 2, 557–566. https://doi.org/10.1038/s41559-017-0459-1

Hirakata, S., Siomi, M.C., 2016. piRNA biogenesis in the germline: From transcription of piRNA genomic sources to piRNA maturation. Biochim. Biophys. Acta - Gene Regul. Mech. 1859, 82–92. https://doi.org/10.1016/J.BBAGRM.2015.09.002

Iki, T., Kawaguchi, S., Kai, T., 2023. miRNA/siRNA-directed pathway to produce noncoding piRNAs from endogenous protein-coding regions ensures Drosophila spermatogenesis. Sci. Adv. 9, eadh0397. https://doi.org/10.1126/sciadv.adh0397

Irles, P., Belles, X., Piulachs, M.D., 2009a. Brownie, a gene involved in building complex respiratory devices in insect eggshells. PLoS One 4, e8353. https://doi.org/10.1371/journal.pone.0008353

Irles, P., Bellés, X., Piulachs, M.D., 2009b. Identifying genes related to choriogenesis in insect panoistic ovaries by Suppression Subtractive Hybridization. BMC Genomics 20. https://doi.org/10.1186/1471-2164-10-206.

Irles, P., Elshaer, N., Piulachs, M.D., 2016. The Notch pathway regulates both the proliferation and differentiation of follicular cells in the panoistic ovary of Blattella germanica. Open Biol. 6. https://doi.org/10.1098/rsob.150197

Irles, P., Piulachs, M.D., 2014. Unlike in Drosophila Meroistic Ovaries, hippo represses notch in Blattella germanica Panoistic ovaries, triggering the mitosis-endocycle

switch in the follicular cells. PLoS One 9, e113850. https://doi.org/10.1371/journal.pone.0113850

Irles, P., Piulachs, M.D., 2011. Citrus, a key insect eggshell protein. Insect Biochem. Mol. Biol. 41, 101–8. https://doi.org/10.1016/j.ibmb.2010.11.001

Jensen, S., Brasset, E., Parey, E., Roest Crollius, H., Sharakhov, I. V., Vaury, C., 2020. Conserved Small Nucleotidic Elements at the Origin of Concerted piRNA Biogenesis from Genes and lncRNAs. Cells 9, 1–20. https://doi.org/10.3390/cells9061491

Kiuchi, T., Koga, H., Kawamoto, M., Shoji, K., Sakai, H., Arai, Y., Ishihara, G., Kawaoka, S., Sugano, S., Shimada, T., Suzuki, Y., Suzuki, M.G., Katsuma, S., 2014. A single female-specific piRNA is the primary determiner of sex in the silkworm. Nature 509, 633–636. https://doi.org/10.1038/nature13315

Kiuchi, T., Shoji, K., Izumi, N., Tomari, Y., Katsuma, S., 2023. Non-gonadal somatic piRNA pathways ensure sexual differentiation, larval growth, and wing development in silkworms. PLoSGenet19 9, e1010912. https://doi.org/10.1371/journal.pgen.1010912

Lambert, M., Benmoussa, A., Provost, P., 2019. Small Non-Coding RNAs Derived from Eukaryotic Ribosomal RNA. Non-Coding RNA 5. https://doi.org/10.3390/NCRNA5010016

Langmead, B., Salzberg, S.L., 2012. Fast gapped-read alignment with Bowtie 2. Nat. Methods 9, 357–9. https://doi.org/10.1038/nmeth.1923

Le Thomas, A., Tóth, K.F., Aravin, A.A., 2014. To be or not to be a piRNA: Genomic origin and processing of piRNAs. Genome Biol. 15, 1–6. https://doi.org/10.1186/gb4154

Livak, K.J., Schmittgen, T.D., 2001. Analysis of relative gene expression data using real-time quantitative PCR and the 2-ΔΔCT method. Methods 25, 402–408. https://doi.org/10.1006/meth.2001.1262

Llonga, N., Ylla, G., Bau, J., Belles, X., Piulachs, M.-D., 2018. Diversity of piRNA expression patterns during the ontogeny of the German cockroach. J. Exp. Zool. Part B Mol. Dev. Evol. 330, 288–295. https://doi.org/10.1002/jez.b.22815

Love, M., Huber, W., Anders, S., 2014. Moderated estimation of fold change and dispersion for RNA-seq data with DESeq2. Genome Biol. 15, 550. https://doi.org/doi:10.1186/s13059-014-0550-8

Martin, M., 2011. Cutadapt removes adapter sequences from high-throughput sequencing reads. EMBnet.journal 17. https://doi.org/10.14806/ej.17.1.200

O’Donnell, K.A., Boeke, J.D., 2007. Mighty Piwis defend the germline against genome

intruders. Cell 129, 37–44. https://doi.org/10.1016/J.CELL.2007.03.028

Oberemok, V. V., Laikova, K. V., Repetskaya, A.I., Kenyo, I.M., Gorlov, M. V., Kasich, I.N., Krasnodubets, A.M., Gal'chinsky, N. V., Fomochkina, I.I., Zaitsev, A.S., Bekirova, V. V., Seidosmanova, E.E., Dydik, K.I., Meshcheryakova, A.O., Nazarov, S.A., Smagliy, N.N., Chelengerova, E.L., Kulanova, A.A., Deri, K., Subbotkin, M. V., Useinov, R.Z., Shumskykh, M.N., Kubyshkin, A. V., 2018. A half-century history of applications of antisense oligonucleotides in medicine, agriculture and forestry: we should continue the journey. Molecules 23. https://doi.org/10.3390/molecules23061302

Pascual, N., Cerdá, X., Benito, B., Tomás, J., Piulachs, M.D., Bellés, X., 1992. Ovarian ecdysteroid levels and basal oöcyte development during maturation in the cockroach Blattella germanica (L.). J. Insect Physiol. 38, 339–348. https://doi.org/10.1016/0022-1910(92)90058-L

Piulachs, M.-D., Pagone, V., Belles, X., 2010. Key roles of the *Broad-Complex* gene in insect embryogenesis. Insect Biochem. Mol. Biol. 40, 468–475. https://doi.org/10.1016/j.ibmb.2010.04.006

Ramos, S., Chelemen, F., Pagone, V., Elshaer, N., Irles, P., Piulachs, M.D., 2020. Eyes absent in the cockroach panoistic ovaries regulates proliferation and differentiation through ecdysone signalling. Insect Biochem. Mol. Biol. 123, 103407. https://doi.org/10.1016/j.ibmb.2020.103407

Roberts, T.., Langer, R., Wood, M.J.A., 2020. Advances in oligonucleotide drug delivery. Nat Rev Drug Discov 19, 673–694. https://doi.org/10.1038/s41573-020-0075-7

Rojas-Ríos, P., Simonelig, M., Rojas-Ríos, P., Simonelig, M., 2018. piRNAs and PIWI proteins: Regulators of gene expression in development and stem cells. Dev. 145. https://doi.org/10.1242/dev.161786

Romaña, I., Pascual, N., Belles, X., 1995. The ovary is a source of circulating ecdysteroids in Blattella germanica. Eur. J. Entomol. 92, 93–103.

Rumbo, M., Pagone, V., Piulachs, M.D., 2023. Diverse functions of the ecdysone receptor (EcR) in the panoistic ovary of the German cockroach. Insect Biochem. Mol. Biol. 156, 103935. https://doi.org/https://doi.org/10.1016/j.ibmb.2023.103935

Senti, K.A., Jurczak, D., Sachidanandam, R., Brennecke, J., 2015. piRNA-guided slicing of transposon transcripts enforces their transcriptional silencing via specifying the nuclear piRNA repertoire. Genes Dev. 29, 1747–1762. https://doi.org/10.1101/GAD.267252.115

Tanaka, A., 1976. Stages in the embryonic development of the German Cockroach, Blattella germanica Linné (Blattaria, Blattellidae). Kontyu 44, 513–525.

Tanaka, E.D., Piulachs, M.D., 2012. Dicer-1 is a key enzyme in the regulation of

oogenesis in panoistic ovaries. Biol. cell 104, 452–61. https://doi.org/10.1111/boc.201100044

Wang, J., Zhang, P., Lu, Y., Li, Y., Zheng, Y., Kan, Y., Chen, R., He, S., 2019. piRBase: a comprehensive database of piRNA sequences. Nucleic Acids Res. 47, D175–D180. https://doi.org/10.1093/NAR/GKY1043

Yamashita, T., Komenda, K., Miłodrowski, R., Robak, D., Szrajer, S., Gaczorek, T., Ylla, G., 2024. Non-gonadal expression of piRNAs is widespread across Arthropoda. FEBS Lett. 2. https://doi.org/10.1002/1873-3468.15023

Ylla, G., Piulachs, M.D., Belles, X., 2017. Comparative analysis of miRNA expression during the development of insects of different metamorphosis modes and germ-band types. BMC Genomics 18, 774. https://doi.org/10.1186/s12864-017-4177-5

Figure legends

Figure 1. piRNA-83679 in ovaries of adult *Blattella germanica*. A. Levels of piRNA-83679 in the small RNA libraries from different developmental stages, including embryos of different ages (days 0, 1, 2, 6 and 13 (E0, E1, E2, E6, E13), nymphs from first (N1), third (N3), fifth (N5) and sixth (N6) instars. Data from transcriptomes from 7-day-old adult ovaries (Ov7) and non-fertilized eggs (NFE) were also included (Ylla et al., 2017). Each value represents the average of normalized counts, conducted using the median-of-ratios method from DESeq2. Data are shown as mean ± S.E.M. (n = 2). **B**. Expression profile of piRNA-83679 in adult ovaries during the first gonadotropic cycle. Data represent copies of piRNA per 1000 copies of *U6*, and are expressed as the mean ± S.E.M. (n = 3). **C.** *In situ* hybridization in late 3-day-old adult ovaries showing the piRNA-83679 localization in the cytoplasm of follicular cells of a BOF. **C'** shows the merged images with the nuclei stained with DAPI. **D.** *In situ* hybridization in follicular cells from 5-day-old adult ovaries. piRNA-83679 labeling accumulates close to the nucleus membrane (arrows). **E.** Subbasal ovarian follicle from a 5-day-old adult, showing the piRNA-83679 labelling in the ooplasm, with increasing labelling towards the oocyte poles (arrowheads); FE: follicular epithelia. N: nucleus. The apical pole is in the top-right. An antisense LNA probe with the piRNA sequence was used, labeled with DIG

at both ends. In C-E, the probe was revealed with a rhodamine-labeled anti-DIG antibody (red). The DNA in the nuclei was stained with DAPI (blue).

Figure 2. Effects of piRNA-83679 depletion in the ovaries of *Blattella germanica*. Newly emerged adult females were treated with ASO or Mock and dissected 7 days later. Images from A-C and E-G correspond to basal ovarian follicles. **A.** Follicular epithelia, from a Mock-treated adult female, showing the follicular cells (FCs) distribution; cells are closing the intercellular spaces; arrows indicate closed intercellular spaces, and arrowheads indicate intercellular spaces that are still open. **B.** F-actin distribution in the basal pole of FCs from a Mock-treated adult female in early chorion stage; the actin fibers in the basal pole of FC are not completely packed. **C.** F-actin distribution in the basal pole of FCs from a Mock-treated adult female in late chorion stage; the F-actin fibers are completely packed giving the FCs a round shape. **D.** Expression levels of piRNA-83679 in 7-day-old *B. germanica* adult ovaries from freshly emerged females that were injected with Mock or ASO. Data represent copies of the piRNA per 1000 copies of *U6*, and are expressed as the mean ± S.E.M. (n = 3). The asterisk indicates statistically significant differences (p = 0.01). **E.** Nuclei from FCs in Mock-treated females, showing the uniformity in size and distribution. **F.** Nuclei from FCs in ASO-treated females, showing the different size and forms. **G.** F-actin distribution in the basal pole of FCs of ASO-treated adult females, showing their disorganization; the F-actin microfilaments were stained with phalloidin-TRITC (red in A, white in B, C and G). DNA was stained with DAPI (blue in A, white in E and F). **H.** Expression of the ecdysteroidogenic genes, *neverland* (*nvd*), *spook* (*spo*), *phantom* (*phm*), *disembodied* (*dib*), and *shadow* (*sad*). **I.** Expression of *shade* (*shd*), *E75A*, *fushi tarazu- f1* (*ftz-f1*), *brownie* (*brw*) and *citrus*. In H and I, data represent copies of mRNA per 1000 copies of *actin-5c* mRNA and are expressed as the mean ± S.E.M. (n = 3-5). The asterisks indicate statistically significant differences respect to Mock-treated: * p = 0.03 (*E75A*); *p = 0.02 (*ftz-f1*); *** p = 0.0003 (*spo*); **** p < 0.0001 (*brw* and *citrus*).

Figure 3. Effects of piRNA-83679 depletion on *Blattella germanica* embryogenesis. **A.** Oothecae from Mock- and ASO-treated females; the later shows the eggs were not well-aligned. **B.** Number of nymphs hatching from oothecae formed by Mock- and ASO-treated females. Each dot represents the total nymphs from one ootheca. Blue dots correspond to well-formed oothecae, and orange dots to defective oothecae. Data are represented as the mean ± S.E.M. (Treated females, n = 27; Control females, n = 24). Asterisks indicate statistically significant differences (** $p < 0.01$). **C.** Fifteen-day-old embryo from Mock-treated females. Segmentation is complete; the sclerotization of mandibles (arrow) and legs (arrowheads) already started. **D-I**: Fifteen-day-old embryo from ASO-treated females. **D.** Embryo similar to controls without sclerotized appendixes. **E**: Embryo with no signs of development. **F.** Embryo with the different body parts differentiated; the appendages have some degree of development; the eyes are not pigmented. **G.** Similar to F but less advanced development; the legs are distinguishable, but the body segmentation was not apparent. **H.** Embryo with a correct body development, however, the head has an abnormal morphology and the dorsal organ is still visible, these modifications determine a miss-localization of the head appendages; in addition, the legs appear to be larger than in controls. **I.** Embryo with complete body segmentation; the head does not have the correct structure; the eyes are correctly pigmented, but the head appendages are not well defined; the legs are short reaching only the first abdominal segments; there is an increase of cells corresponding to the fat body that appeared like white dots.

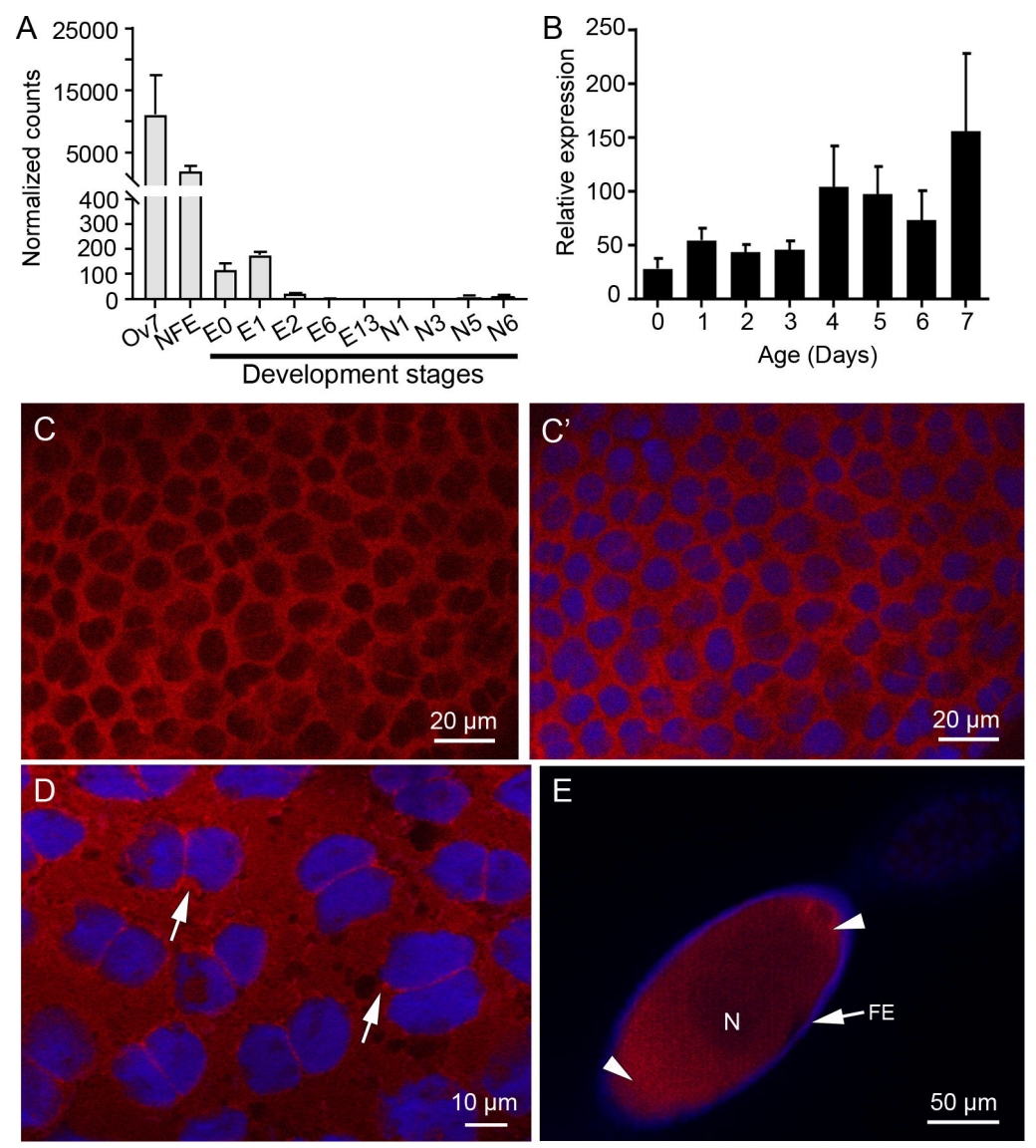
A
Normalized counts
25000
15000
5000
400
300
200
100
0
Ov7
NFE
E0
E1
E2
E6
E13
N1
N3
N5
N6
Development stages
B
Relative expression
250
200
150
100
50
0
0
1
2
3
4
5
6
7
Age (Days)
C
20 µm
C'
20 µm
D
10 µm
E
N
FE
50 µm

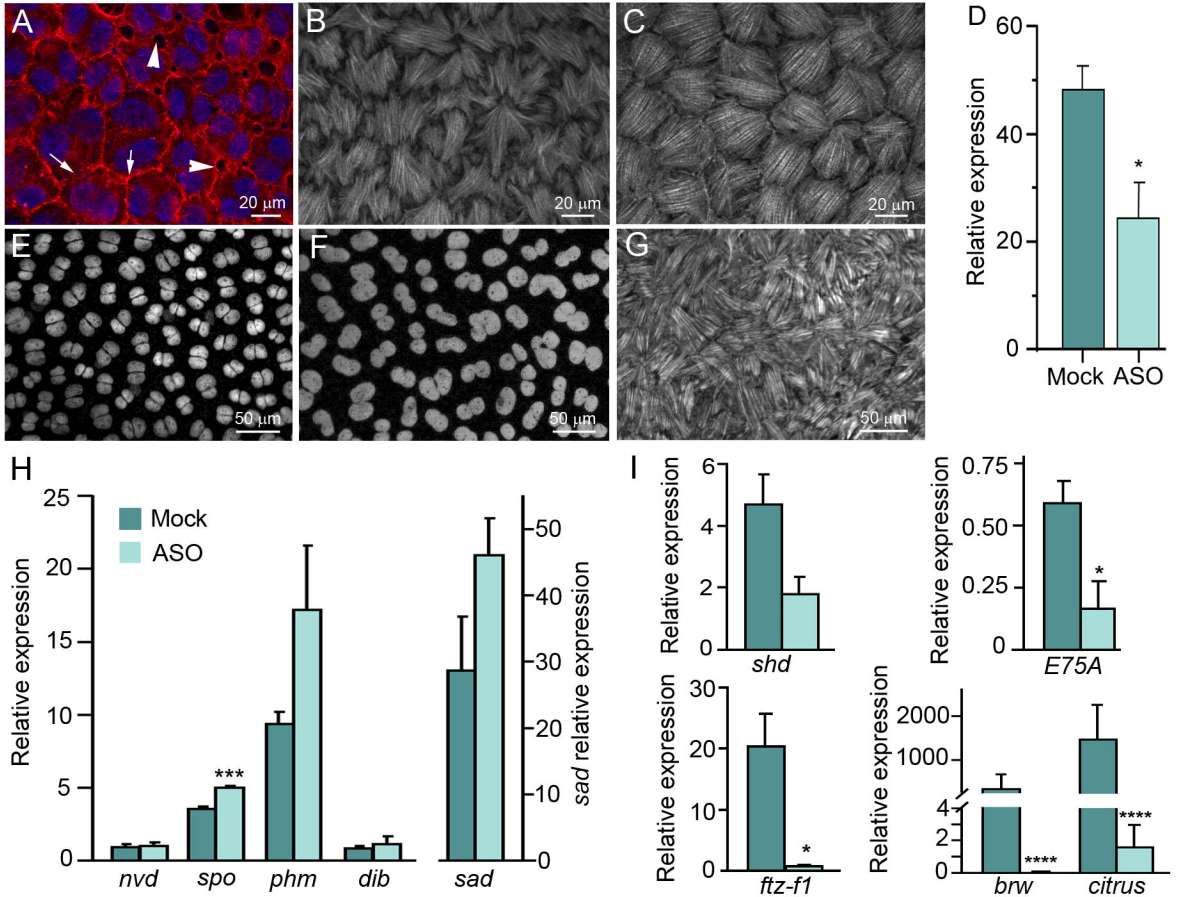
A
20 µm
B
20 µm
C
20 µm
D
Relative expression
60
40
20
0
*
Mock
ASO
E
50 µm
F
50 µm
G
50 µm
H
Mock
ASO
Relative expression
25
20
15
10
5
0
***
nvd
spo
phm
dib
sad
sad relative expression
50
40
30
20
10
0
I
Relative expression
6
4
2
0
shd
0.75
0.50
0.25
0
*
E75A
30
20
10
0
*
ftz-f1
2000
1000
4
2
0
****
****
brw
citrus

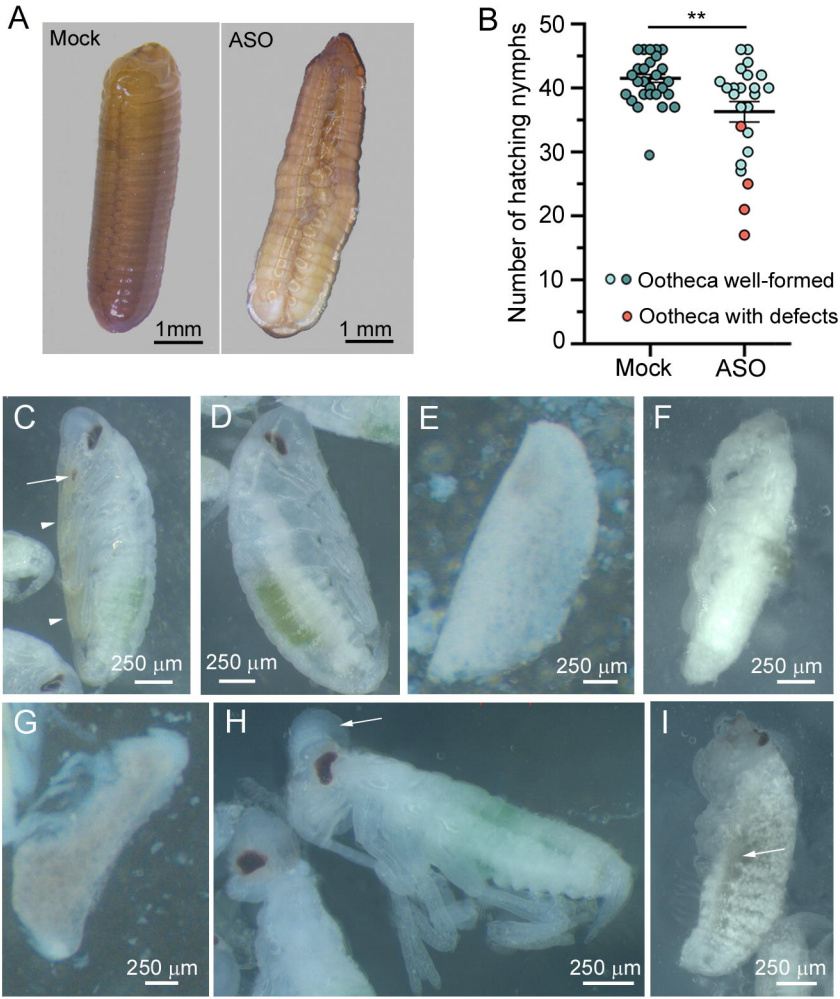
A
Mock
ASO
1mm
1 mm
B
Number of hatching nymphs
50
40
30
20
10
0
**
Ootheca well-formed
Ootheca with defects
Mock
ASO
C
D
E
F
G
H
I
250 μm